

Gas bubble formation and velocity measurements inside the narrow gap flow of a journal bearing model

Matthias Nobis^{1*}, Peter Reinke² and Marcus Schmidt²

¹ University of Applied Sciences Zwickau, Faculty of Automotive Engineering, Germany

² University of Applied Sciences and Arts Hildesheim/Holzminde n/Göttingen, Faculty of Natural Sciences
and Technology, Germany

*Matthias.Nobis@fh-zwickau.de

Abstract

In order to get more knowledge about the flow conditions inside the gap of crankshaft main bearings, a special model test rig was developed. The design is based on similarity laws resulting in a scaled model including the detailed local bearing geometry of a genuine crankshaft main bearing. Additionally, means were developed to produce a simplified shaft displacement curve. Shaft displacement is a characteristic feature of combustion engines. During the operating cycle the crankshaft performs radial movements resulting in an unsteady eccentricity between shaft and liner. The individual operating cycle of any crankshaft bearing can show critical conditions of eccentricity in combination with its change rate that are prone to cavitation. Thus, the displacement mechanism of the model experiment must target these critical conditions to yielding a flow field similar to the real crankshaft main bearing.

The model experiment is constructed from transparent acrylic glass that allows the access by means of optical measuring methods to investigate the flow field. Color visualization gives a global impression of the complexity of the flow problem. In addition, at selected locations inside the flow field laser-optical measurements produce velocity distributions in great detail. Moreover, experiments with a two-phase fluid reveal the bubble formation during the cavitation process. The combination of these experimental data is in good agreement with the validated numerical results.

1 Introduction

The flow inside the gap of a hydrodynamically lubricated journal bearing has been subject of many investigations since the 19th century. Osborne Reynolds (1886) laid the foundation for the mathematical description of the processes in the lubricating gap with his Theory of Lubrication. State-of-the-art simulation tools make use of this reduced two-dimensional theory during the design process of journal bearings. There are however, particular flow conditions where the application of two-dimensional methods is at the most limited or even giving false results. For example, transitional three-dimensional flow occurs adjacent to the local bearing geometry (grooves, feed holes etc.) and in the event of cavitation. These three-dimensional flows are subject of current research and the work on hand focuses particularly on a new experimental approach.

The experimental investigation of the lubrication flow inside a journal bearing, between the rotating shaft and the stationary liner represents a challenging problem, even under the application of state-of-the-art measuring technology. Moreover, the validation of newly developed three-dimensional computation methods requires information from the inside of the flow field which falls beyond the reach of traditional measurement means applied to original bearings. Traditionally, experiments were carried out obtaining the bearing loads externally as well as measuring pressure distributions and shaft displacement by tapping the liner with micro probes. These techniques were applied inside fired engines or at special bearing test rigs

producing good results for the general understanding of journal bearing characteristics but fail to reach inside the flow field, entirely.

2 Experimental Setup

The geometry of the model test rig is derived from the geometry of a real journal bearing liner. At a scale of 1:3 all relevant dimensions were transferred to the bearing model in Figure 1. The shaft and housing of the model are made of transparent acrylic glass to provide optical access into the narrow lubrication gap. The housing can be fixed on the linear profile guide in a targeted eccentric basic position relative to the shaft. In summary three stepping motors are installed. The first one rotates the shaft. With the second one turns the housing, which is mounted on a turntable. The third stepping motor drives a cranking mechanism with a freely selectable speed ratio synchronous to the drive of the shaft. The cranking mechanism generates an oscillating movement of the housing in relation to the shaft. It has an adjustable slider for determining the amplitude of the oscillating movement. Thus, it is possible to adjust the maximum dynamic eccentricity. A micrometer screw guarantees exact positioning of the slider.

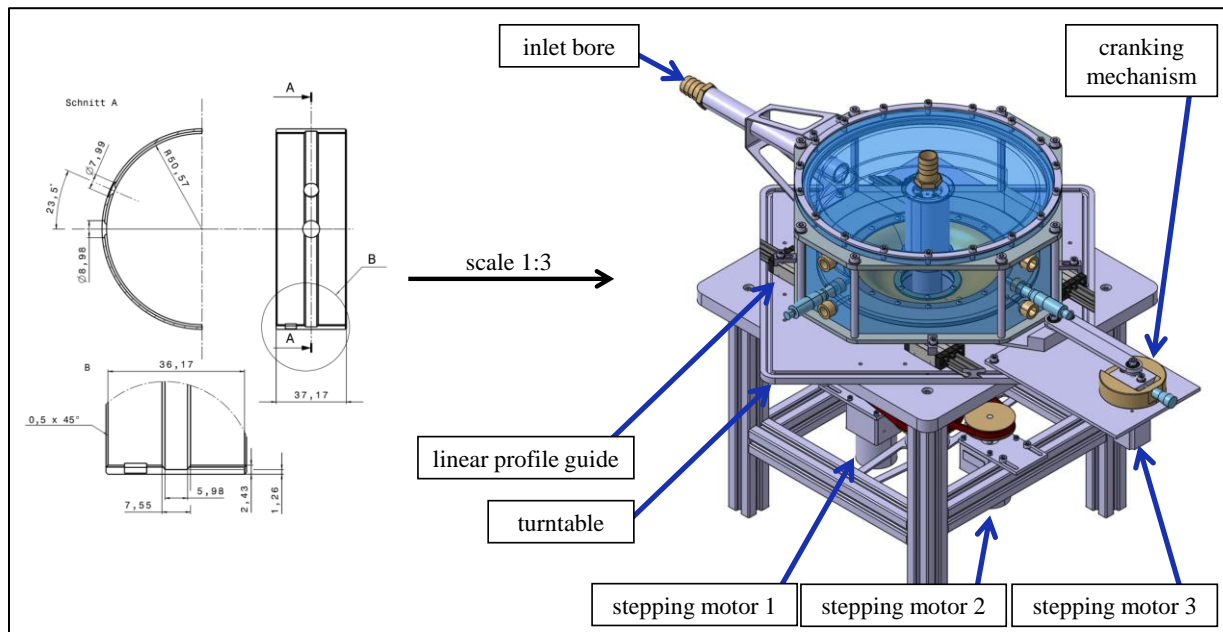


Figure 1: Real journal bearing liner (left) from Nobis et al. (2012) and journal bearing model (right) from Nobis et al. (2016)

Transient gap width conditions can be generated by means of a dynamic displacement of the bearing housing. Thus, it is possible to reproduce the load dependent shaft displacements in a real journal bearing of an internal combustion engine in a very simplified form. These relative displacements in radial direction between the shaft and the housing are the initial point for quench flows in the lubrication gap. There is no demand for copying the exact shaft displacement track of a selected operating point of an internal combustion engine. From the point of view of flow studies there is a need to ensure the principal generation of a quench flow in a reproducible manner.

For the measurement of flow velocities inside the lubrication gap, a LDV is used. It is positioned axially above the bearing model and mounted on a two-way traverse system. This allows a very exact positioning of the measuring volume in axial and radial direction inside the gap. In order to realize different angular measuring positions the turntable together with the bearing housing will be rotated gradually. With this type of alignment the circumferential component of the local flow velocity can be measured.

3 Geometrical Parameters

Figure 2 shows a schematic longitudinal and cross section through the journal bearing model with the associated geometrical parameters. The position of the inlet bore in the housing is defined by the angle φ_B starting from the widest gap. The rotation angle of the shaft is given relative to the angular position of the inlet bore. By definition at a rotation angle of 0° the outlet bore of the shaft is aligned with the inlet bore of the housing.

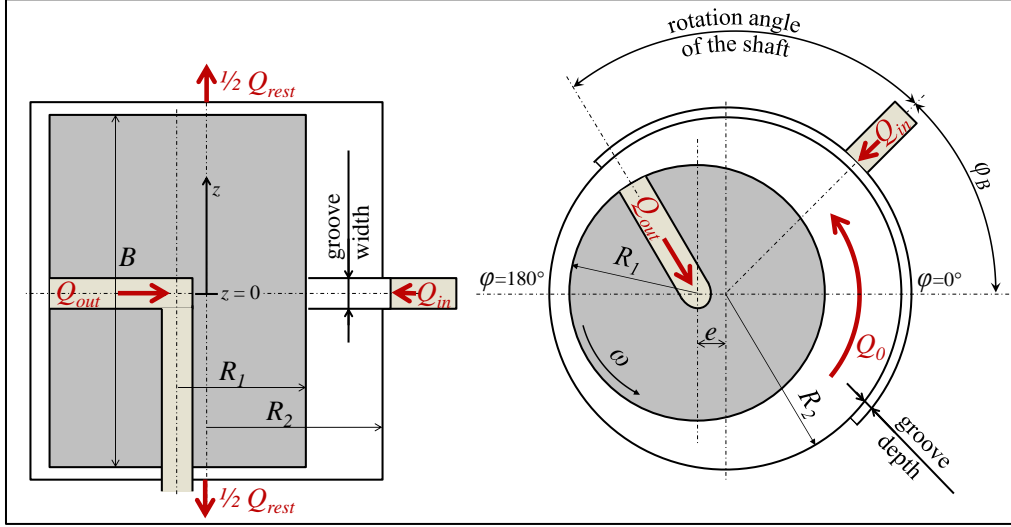


Figure 2: Schematic sections through the journal bearing model

$$H_0 = R_2 - R_1 \quad (1)$$

$$\Psi = \frac{H_0}{R_1} \quad (2)$$

$$\varepsilon = \frac{e}{H_0} \quad (3)$$

$$Q_0 = \frac{1}{2} \cdot U_1 \cdot B \cdot H_0 \quad (4)$$

$$U_1 = \omega \cdot R_1 \quad (5)$$

$$\alpha_{in} = \frac{Q_{in}}{Q_0} \quad (6)$$

$$\alpha_{out} = \frac{Q_{out}}{Q_{in}} \quad (7)$$

$$Re = \frac{U_1 \cdot H_0}{\nu} \quad (8)$$

The given equations (1) to (3) define in detail the average clearance (1), the relative gap width (2) and the relative eccentricity (3). The relative eccentricity ε sets the distance e between the center axes of shaft and housing in relation to the average clearance H_0 . According to the explanations in the section Experimental Setup the eccentricity is composed of two parts. The first part is given by the basic eccentric position of the housing compared to the shaft and is defined as the static eccentricity. The second part is caused by the oscillating movement of the housing and is therefore referred as the dynamic eccentricity. The following equations (4) to (7) define the inner volumetric flow rate caused by the rotation of the shaft (4), the circumferential velocity at the surface of the rotating shaft (5) and volumetric flow ratios (6) respectively (7). According to equation (8), the circumferential velocity U_1 and the average clearance H_0 are used to determine the Reynolds number in the lubrication gap for an adjusted rotational speed. According to Küntschner et al. (2014) especially for crankshaft main bearings the relative gap width is usually within a range of $\Psi = 0,1\%$. Depending on the viscosity of the engine oil and the engine speed the range of the Reynolds number is extended from $Re = 20$ to $Re = 300$.

4 Visualization of gas bubble formation

In the crankshaft main bearings of an internal combustion engine are different types of cavitation present. Nemeč (1975) defined four basic types of cavitation. There are the so called impact cavitation, the suction cavitation, the exit cavitation and the flow cavitation. Every type has a own special cause and a different visual appearance of the resulting bearing damage. In the present paper primarily the formation of gas bubbles in context with the impact cavitation is discussed.

Compared to a real journal bearing the model test rig has a considerably larger relative gap width of $\Psi = 2,462\%$. As one result, no matter how large the adjusted eccentricity is, the pressure gradients in the lubrication gap will be comparatively low. The acrylic glass used for the main components limits the allowable pressure gradients anyway to a small area near the ambient pressure. However, the vapor pressure of new engine oil without contaminants is sometimes below 1 Pa absolute pressure. Together with the requirement that a clear liquid is necessary for the observation of bubble formation in deeper layers of fluid, a replacement fluid adapted to the boundary conditions must be used.

Water which is enriched with carbon dioxide is well suited for this purpose. The amount of carbon dioxide which can be dissolved in water depends on temperature and pressure according to Diamond et al. (2003). With an enrichment of the water up to the respective saturation limit, a small pressure reduction causes the dissolution of carbon dioxide. Thus, the dissolved carbon dioxide releases the water in areas of lower pressure and forms visible gas bubbles. The outgassing of carbon dioxide from water is a process of the uncritical gas cavitation. According to Sun and Brewe (1991) the erosion of material from the bearing housings is primarily caused by steam cavitation. However, this method is suitable to visualize bubble formation, if the analogy between the pressure and temperature-dependent CO_2 -saturation limit in the model experiment and vapor cavitation in real bearings is carefully observed.

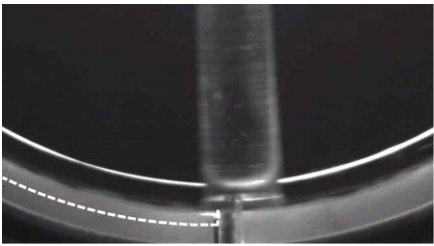
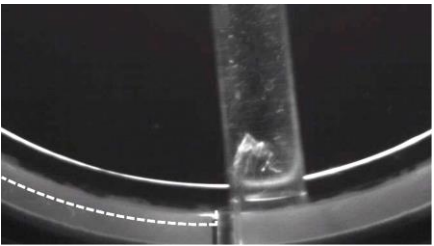
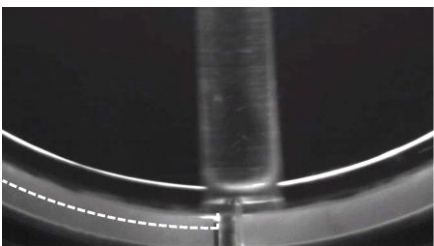
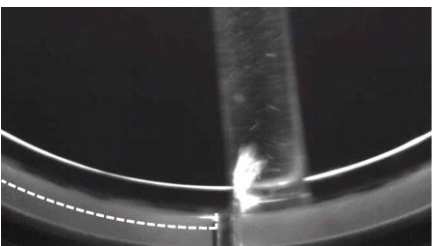
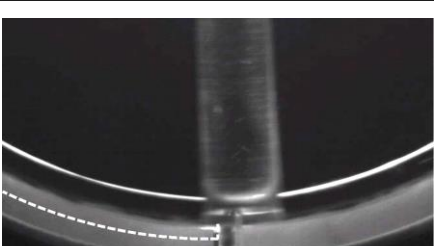
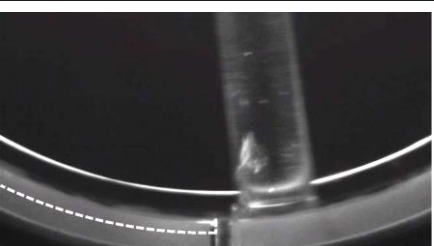
<p>rotation angle of the shaft 182°</p> 	<p>rotation angle of the shaft $183,4^\circ$</p>  <p> $n = 1/s$ $Q_{in} = 14,7 \text{ l/min}$ $\alpha_{in} = 133 \%$ $Re_{local} = 157$ $\epsilon_{stat} = 95 \%$ $\epsilon_{dyn} = 0 \%$ </p>
	 <p> $n = 2/s$ $Q_{in} = 14,7 \text{ l/min}$ $\alpha_{in} = 66,5 \%$ $Re_{local} = 314$ $\epsilon_{stat} = 95 \%$ $\epsilon_{dyn} = 0 \%$ </p>
	 <p> $n = 1/s$ $Q_{in} = 11,0 \text{ l/min}$ $\alpha_{in} = 50 \%$ $Re_{local} = 314$ $\epsilon_{stat} = 95 \%$ $\epsilon_{dyn} = 0 \%$ </p>

Figure 3: Visualized bubble formation in the outlet bore of the shaft from Nobis (2017)

A membrane contactor is used to control the insertion of carbon dioxide into the water. In the membrane contactor numerous semi-permeable hollow fiber membranes provide a non-dispersed solution of carbon dioxide in the water. By means of pressure reducer, a targeted pressure ratio between the liquid and gas side in the membrane contactor can be set. The adjustment of the pressure ratio defines the amount of carbon dioxide to be dissolved in the water. The higher the concentration of dissolved carbon dioxide in the water, the more gas bubbles will be generated in local low pressure areas. The optical recording of the gas bubble formation process is carried out with a high-speed camera with focus in axial direction.

The images in Figure 3 were taken with a frame rate of 250 fps at various boundary conditions. The documented bubble formation processes in the outlet bore of the shaft are caused by the superposition of two mechanisms. When the outlet bore moves out of the groove area, an abrupt reduction of the outlet cross section occurs. Hence, there is an eminent acceleration of the fluid which leads to a significant increase of the local flow velocity and consequently to a local decrease of the static pressure. Another consequence of the sudden reduction of the outlet cross section is a prompt reduction of the volumetric flow rate. The inertia of the flowing liquid in the outlet bore creates a suction effect for a short time and the static pressure is lowered again. In combination, both of these relationships reduce the static pressure briefly to a level at which the carbon dioxide releases the water and forms visible gas bubbles. The comparison between the three images on the right side in Figure 3 shows that a higher rotational speed or a higher volumetric flow rate leads to a significantly stronger bubble formation.

It is already known that the risk of cavitation can be reduced by increasing the static pressure. However, as the comparison of the images in Figure 3 shows, it is nonproductive to counteract the impact cavitation in a journal bearing with an increase in the oil supply pressure which goes along with increasing the supplied volumetric flow rate. The achieved increase in the global pressure level is always accompanied by the increase of local flow velocities. Together with the enhancement of the local suction effects in the outlet bore, increasing the oil supply pressure tends to be counterproductive. In this case, changes in the structural design of the groove end must rather be carried out. Garner et al. (1980) propose a tangential groove end as a preventive procedure. In consequence the reduction of the outlet cross section is less abrupt when the outlet bore of the shaft leaves the groove area. The result is a significantly reduced tendency to impact cavitation.

4 Velocity measurements in the gap

The velocity profiles in Figure 4 illustrate the differences in the flow field between an adjustment with only static eccentricity (case 1) and an adjustment with only dynamic eccentricity (case 2) with otherwise identical setting parameters. In both cases there are transient flow conditions which are effected by the interaction of the Couette flow, the incoming flow through the inlet bore, the outgoing flow through the outlet bore in the rotating shaft and especially in case 2 the additional quench flow caused radial movement of the housing. Hence, the shown velocity profiles should be understood as a snapshot at a selected time step. The exact course of the eccentricity for each case is given in the upper diagram of Figure 4. For case 2 the angular position of the narrowest gap changes between $\varphi = 0^\circ$ and $\varphi = 180^\circ$. Accordingly the oscillation of the housing is in the axial direction of the inlet bore.

For the selected time step respectively rotation angle of the shaft of 1° there are nearly the same gap conditions for the two cases. However, in case 2 the crank drive has passed the top dead center and the gap will become smaller at $\varphi = 0^\circ$ during the following time steps. Consequently a quench flow into the direction of the increasing gap area at $\varphi = 180^\circ$ is initiated and deforms the velocity profile in a kind of less deflection. In this context the back flow area is comparatively decreased significant for this time step. The simplified radial movement of the housing leads to knowledge about the influences of the quench flow and causes at least temporarily flow conditions which are common for the flow field inside the lubricating gap of unsteady loaded crank shaft main bearings. From the point of view of the three-dimensional flow simulations the discussed case 2 is a very complex flow problem for which no practicable solutions with reasonable calculation times are available today. Thus, a comparison between numerical and experimental velocity profiles for the transient case remains open.

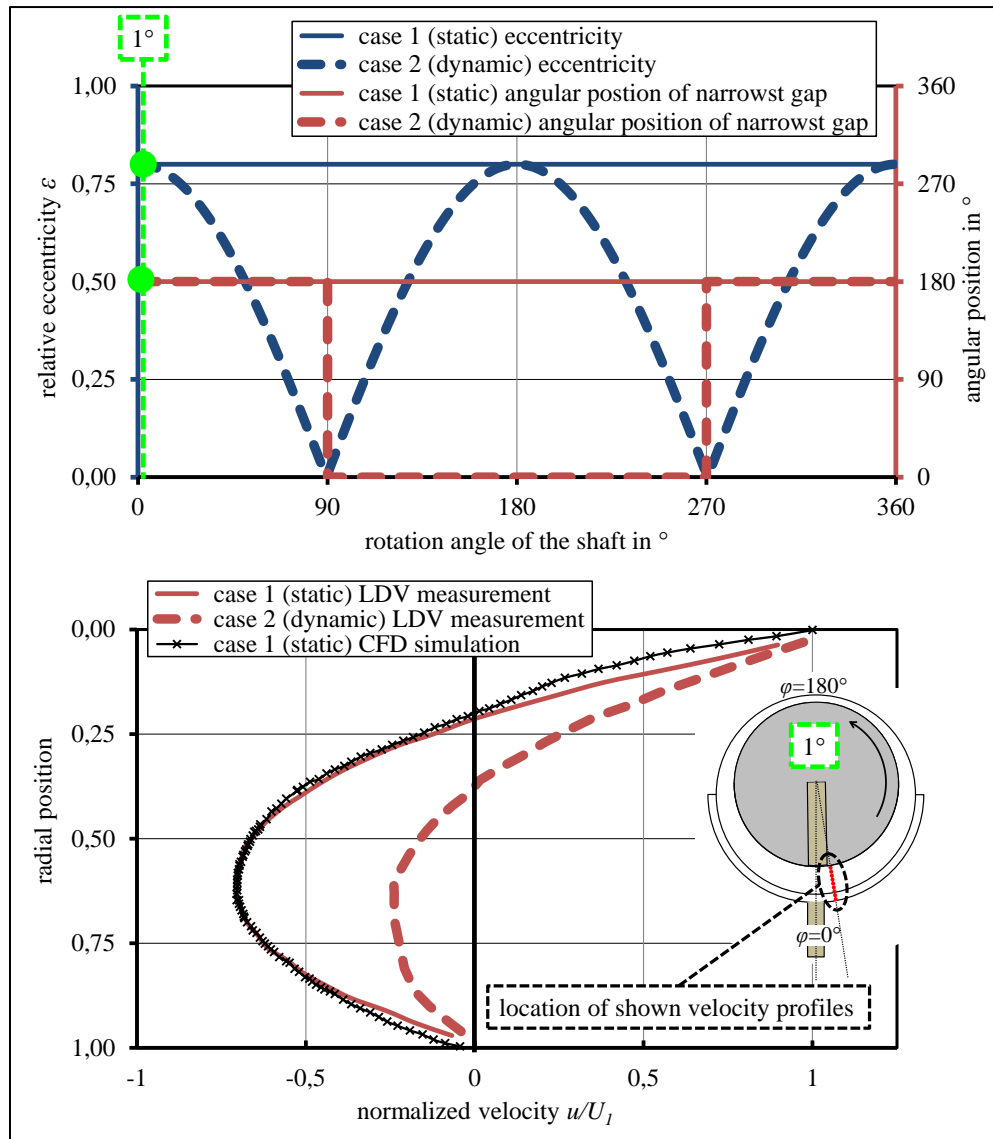


Figure 4: Comparison of velocity profiles by a rotation angle of the shaft of 1° ,

$$\Psi = 2,462\%, \quad \varphi = 8,96^\circ, \quad \alpha_{in} = 50\%, \quad \alpha_{out} = 100\% \quad \text{and} \quad Re = 35$$

in case 1 only with a static eccentricity $\varepsilon_{stat} = 80\%$ and $\varepsilon_{dyn} = 0\%$

in case 2 only with a dynamic eccentricity $\varepsilon_{stat} = 0\%$ and $\varepsilon_{dyn} = 80\%$

4 Conclusion

The present work deals with experimental and numerical investigations of the flow field inside the lubricating gap of a crank shaft main bearing model. A transparent bearing model is used to visualize the formation of gas bubbles during impact cavitation and allows optical access into the flow to apply LDV. Moreover, the bearing model includes typical features of genuine crank shaft bearings such as an oil groove on the inside of the housing and an outlet bore inside the shaft. In addition to the geometrical similarity, the model experiment is fitted with an actuator that creates a movement of the housing which can be calibrated to reproduce specific gap width changes, which are similar to critical shaft displacement conditions that occur during the load cycle of combustion engines. The model fluid in the experiment is water enriched with carbon dioxide, which shows analogous cavitation behavior within characteristic pressure boundaries for the case of the impact cavitation. The experimental results of this work include velocity profiles of the transient flow due to the outgoing flow through the bore in the rotating shaft and

due to gap width changes caused by the displacement of the housing as well as flow visualization, bubble formation and bubble transport. The comparison between experimental and numerical results shows excellent agreement. For future work the visualization of the bubble formation of other types of cavitation which are typical for crank shaft main bearings will be carried out. For this purpose the acceleration rate of the housing movement especially at high eccentricity needs particular attention. From the point of view of the numerical flow simulation there remains work to reproduce the case where the housing is moved by means of the actuator resulting in a sinusoidal gap width variation. The presence of a variable eccentricity with simultaneous outflow through the outlet bore of the rotating shaft creates very high demands on the numerical model. The obtained measurement results can also be used as a basis for comparison for future work in the field of three-dimensional calculation of the flow inside lubricating gaps.

4 Nomenclature

B	breadth of the bearing	Re	Reynolds number
e	eccentricity	U_1	circumferential velocity of the shaft
h	local gap width	$\alpha_{in}, \alpha_{out}$	ratios of volumetric flow rates
H_0	average clearance	φ	angle
Q_0	inner volumetric flow rate	φ_B	angle of inlet bore
Q_{in}	incoming volumetric flow rate	ν	kinematic viscosity
Q_{out}	vol. flow rate over outlet bore in shaft	ε	relative eccentricity
Q_{rest}	vol. flow rate over axial ends	ψ	normalized clearance
R_1	radius of the shaft	ω	rotational speed of the shaft
R_2	radius of the housing		

References

- Diamond L W, Akinfiyev N N (2003) Solubility of CO₂ in Water from -1,5 to 100°C and from 0,1 to 100 MPa: evaluation of literature data and thermodynamic modelling. *Fluid Phase Equilibria* 208, pp. 265 - 290
- Garner D R, James R D, Warriner J F (1980) Cavitation erosion damage in engine bearings: theory and practice. *Journal of Engineering for Power*, Vol. 102, pp. 847 - 857
- Küntschner V, Hoffmann W (2014) Kraftfahrzeugmotoren. *Vogel Buchverlag, Würzburg*, 5. Auflage, pp. 1165 - 1336
- Nemec K L (1975) Erkenntnisse zur Problematik der Zuverlässigkeits- und Lebensdauererhöhung von Diesel-Motoren-Gleitlagern. *Maschinenbautechnik* 24, pp. 112 - 116
- Nobis M (2017) Experimentelle Untersuchung der Spaltströmung in einem Modell eines Kurbelwellenhauptlagers. *Dissertation, BTU Cottbus-Senftenberg*
- Nobis M, Reinke P, Schmidt M, Egbers C (2016) Einfluss der Wellenverlagerung auf das Strömungsfeld im Schmierspalt eines Gleitlagermodells. *Lasermethoden in der Strömungsmesstechnik*, pp. 29-1 - 29-11
- Nobis M, Stücke P, Schmidt M, Riedel M, Egbers C, Herzog N, Gorenz P, Christl A (2012) Experimentelle und numerische Untersuchung der instationären Strömung im Schmierspalt eines Gleitlagermodellprüfstandes. *Lasermethoden in der Strömungsmesstechnik*, pp. 20-1 - 20-10
- Reynolds O (1886) On the theory of lubrication and its application to Mr. Beauchamp Tower's experiments including an experimental determination of the viscosity of olive Oil. *Philosophical Transactions of the Royal Society of London*, Vol. 177, pp. 157 - 234
- Sun D C, Brewster D E (1991) Two reference time scales for studying the dynamic cavitation of liquid films. *NASA Technical Memorandum* 103673